Curvature-Dependent Two-Equation Model for Prediction of Turbulent Recirculating Flows

S. W. Park* and M. K. Chung†
Korea Advanced Institute of Science and Technology, Seoul, South Korea

A new curvature-dependent two-equation model is proposed for prediction of turbulent recirculating flows. A time scale of third-order diffusive transport correlations in the k-ϵ equations is assumed as a function of the time scale ratio between a velocity time scale and a curvature time scale, the latter being derived from the analogy between buoyancy and streamline curvature effects on turbulence. The model coefficient of the destruction term in the ϵ equation is also modified by the time scale ratio in order to incorporate the streamline curvature effect on the decay rate of turbulent kinetic energy. The new curvature-dependent two-equation model is applied to various kinds of turbulent recirculating flows. It has been found that better prediction accuracy can be obtained for both velocity and pressure fields by the present model than by previous curvature correction methods.

Nomenclature

a, b	= model constants for composite time scale
C_p	= wall static pressure coefficient
C_μ, $C_{\epsilon 1}$, $C_{\epsilon 2}$	= coefficients in turbulence model
D, H	= channel and step height
k	= turbulent kinetic energy
L_u, L_d	= lengths of upstream and downstream boundaries
P	= static pressure
p	= pressure fluctuation
T	= normal fence thickness
U	= mean velocity
u	= turbulent fluctuating velocity
X, Y	= Cartesian coordinates
α	= model constant for inlet condition
δ	= boundary-layer thickness
δ_{ij}	= Kronecker delta
ϵ	= dissipation rate of turbulent kinetic energy
μ	= viscosity
μ_t	= turbulent viscosity
ν_t	= turbulent kinematic viscosity
ρ	= density
σ_k, σ_ϵ	= turbulent Prandtl number for k and ϵ, respectively
τ_c	= curvature time scale
τ_v	= velocity time scale

Subscripts

i, j	= tensor notations
min	= minimum value
0	= reference value

Superscripts

$(\ )'$	= modified value
$(\bar{\ })$	= conventional time average

Introduction

TURBULENT recirculating flow consists of many flow regions such as separated free shear layer, recirculating flow region, reattachment region, and redeveloping region. Since the flow characteristics are significantly different depending on the flow region, previous computational models have invariably shown a zonal dependency of the prediction accuracy. For example, the standard two-equation model yields good prediction in the redeveloping region, but it overpredicts the velocity profile near the wall in the recirculating flow region.[1] But higher-order turbulence models, such as the algebraic stress model, yield good prediction on the mean velocity profile in the recirculating flow region,[1,2] whereas they underpredict the velocity profiles in the redeveloping region.

Development of the turbulence structure is highly sensitive to the streamline curvature in a plane of the mean shear.[3,4] First, the turbulent shear stresses and intensities are reduced by streamline curvature when the angular momentum of the fluid element increases in the direction of the radius of streamline curvature (i.e., convex curved), and they are increased when the angular momentum decreases with the radius of streamline curvature (i.e., concave curved). In other words, the decay rate of the turbulent Reynolds stresses depends on the convexity or concavity of the streamline curvature. Second, the response of the turbulence structure to the convex curvature is much more rapid than that to the concave curvature. Third, it has been found by Bradshaw et al.[3-5] that the time response of the third-order correlations to the convex streamline curvature is slower than that of the second-order correlations. Accordingly, computational closure schemes must take into account these experimental observations in the model equations. However, none of the previous curvature correction methods explicitly reflect these physical natures in the formulation of the closure models.[6-10]

Another drawback of one of the most popular curvature correction models is that, since the curvature corrected eddy viscosity is substituted into every model term that contains the Reynolds shear stresses in the equations for turbulent kinetic energy k and its rate of dissipation ϵ, the effect of the streamline curvature is, consequently, unreasonably overemphasized in the model equations.

From the foregoing considerations, the present study is aimed at developing a more realistic curvature-dependent two-equation model that explicitly includes these curvature effects on turbulence.

Accuracy of the proposed model in this study is assessed by comparison between predictions and experimental data on the following two-dimensional recirculating flows: 1) flow over a surface-mounted thick fence measured by Moss and Baker[11] using the pulsed wire anemometer, 2) a surface-mounted thin-fence flow measured by Fraser and Siddig[12] with the laser Doppler anemometer, 3) flow over a backward-facing step which was measured by Eaton[13] with the pulsed wire

Received Feb. 12, 1987; revision received April 2, 1988.

*Currently, Senior Researcher, Korea Standards Research Institute, Taedok Science Town, Chungnam, South Korea.

†Professor, Department of Mechanical Engineering.

anemometer, and 4) a front-facing step flow studied by Moss and Baker[11] with the pulsed wire anemometer.

Mathematical Model

The governing equations for steady-state turbulent flows can be written in Cartesian tensor notation as follows:

Continuity

$$\frac{\partial \rho U_i}{\partial X_i} = 0 \tag{1}$$

Momentum:

$$\frac{\partial \rho U_i U_j}{\partial X_j} = -\frac{\partial P}{\partial X_i} + \frac{\partial}{\partial X_j}\left[\mu\left(\frac{\partial U_i}{\partial X_j} + \frac{\partial U_j}{\partial X_i}\right) - \rho\overline{u_i u_j}\right] \tag{2}$$

where U_i and u_i are, respectively, the mean and fluctuating parts of the velocity, P is the mean static pressure, and ρ and μ represent the fluid density and dynamic viscosity, respectively.

The Reynolds stresses in Eq. (2) are generally modeled through Boussinesq's eddy viscosity assumption, which expresses the Reynolds stresses with the mean strain rates by the relation $-\overline{u_i u_j} = \nu_t(U_{i,j} + U_{j,i}) - 2k\,\delta_{ij}/3$. In the so-called two-equation model, the turbulent eddy viscosity ν_t is approximated by $\nu_t = C_\mu k^2/\epsilon$, where k and ϵ are obtained by solving

$$\frac{Dk}{Dt} = -\frac{\partial}{\partial X_j}\left[\overline{u_j\left(\frac{u_i u_i}{2} + \frac{p}{\rho}\right)}\right] - \overline{u_i u_j}\frac{\partial U_i}{\partial X_j} - \epsilon \tag{3}$$

$$\frac{D\epsilon}{Dt} = \frac{\partial}{\partial X_j}(-\overline{\epsilon' u_j}) - C_{\epsilon 1}\frac{\epsilon}{k}\overline{u_i u_j}\frac{\partial U_i}{\partial X_j} - C_{\epsilon 2}\frac{\epsilon^2}{k} \tag{4}$$

The model constants C_μ, $C_{\epsilon 1}$, and $C_{\epsilon 2}$ are usually taken as 0.09, 1.43, and 1.92, respectively.

The conventional models for the third-order transport terms, the first terms on the right-hand sides of Eqs. (3) and (4), are the simple gradient diffusion models. The time scale for such third-order transports has been approximated by a single velocity time scale $\tau_v = k/\epsilon$, which is independent of the streamline curvature. But it has been found that the third-order transport must have a curvature-dependent time scale different from the velocity time scale.[3,14] In the present study, such streamline curvature effect on the third-order correlation is modeled by devising a curvature time scale τ_c for the third-order transport mechanism from the analogy between buoyancy and streamline curvature effects on turbulence. Details of the derivation procedure are described by Chung et al.[14]

The final model forms for the third-order transport terms are

$$-\overline{u_j\left(\frac{u_i u_i}{2} + \frac{p}{\rho}\right)} = \frac{C_\mu}{\sigma_k}\left(\frac{1}{1 + a\tau_v/\tau_c}\right)\frac{k^2}{\epsilon}\frac{\partial k}{\partial X_j} \tag{5}$$

$$-\overline{\epsilon' u_j} = \frac{C_\mu}{\sigma_\epsilon}\left(\frac{1}{1 + a\tau_v/\tau_c}\right)\frac{k^2}{\epsilon}\frac{\partial \epsilon}{\partial X_j} \tag{6}$$

The model constant a was given to be $a = 0.12$ by Chung et al.[14]

The recent experiments by Bradshaw et al.[3-5] reveal that length scale is decreased significantly after application of convex streamline curvature. The reduction in the length scale by the convex streamline curvature implies that the turbulent kinetic energy decays at a faster rate. Therefore, the decay rate constant $C_{\epsilon 2}$ of the destruction term in the ϵ equation must be modeled as a function of the curvature time scale. The most convenient form that represents such an effect of the streamline curvature on the decay rate is found to be

$$C'_{\epsilon 2} = C_{\epsilon 2}/(1 + b\tau_v/\tau_c) \tag{7}$$

where the model constant b is determined to be $b = 0.50$ by computer optimization.

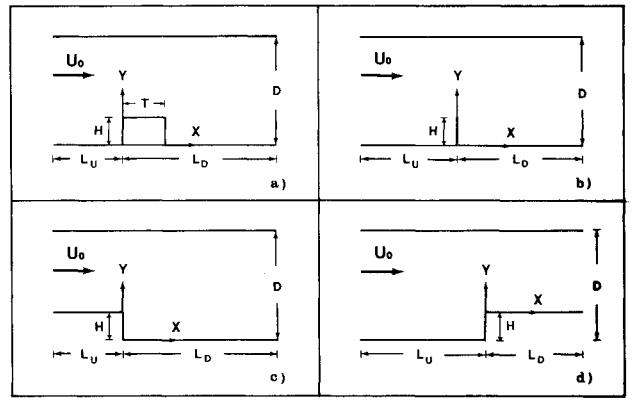

Fig. 1 Schematics of various two-dimensional recirculating flows: a) thick-fence flow, b) thin-fence flow, c) backward-facing step flow, d) front-facing step flow.

Table 1 Geometrical dimensions and inlet conditions[a]

Parameters	Thick fence[11]	Thin fence[12]	BFS[13]	FFS[11]
H, m	0.076	0.03	0.051	0.076
D, m	$11H$	$6.67H$	0.127	$11H$
T, m	$2H$	$\ll 1$	—	—
L_u, m	$10H$	$10H$	$5H$	$12H$
L_d, m	$28H$	$32H$	$33H$	$30H$
δ, m	$0.1H$	$0.667H$	$0.012H$	$0.1H$
U_0, m/s	10.0	3.7	11.65	10.0
$\sqrt{\overline{u^2}}/U_0$, %	0.6	1.0	—	0.6

[a] δ = inlet boundary-layer thickness, U_0 = reference inlet velocities, $\sqrt{\overline{u^2}}/U_0$ = turbulent intensity of the inlet flow, BFS = backward-facing step, FFS = front-facing step.

Boundary Conditions and Solution Procedure

Figure 1 illustrates four different kinds of recirculating flow configurations studied in the present work. The relevant flow parameters are included in the figure. The inlet boundary is located sufficiently far upstream of the obstacle so that its presence is not felt, and the outlet is located sufficiently far downstream from the reattachment point. The lower and upper boundaries correspond to the wind-tunnel walls. Geometric dimensions and inlet conditions are given for each case in Table 1.

No-slip boundary conditions are imposed on the mean velocities along the walls, and the streamwise gradients of all unknown variables are assumed to vanish at the outlet plane. At the inlet plane, streamwise mean velocity profiles are given by those from the experimental data. The inlet profiles for k and ϵ are estimated from

$$k = \alpha U^2 \tag{8a}$$

$$\epsilon = k^{3/2} C_\mu^{3/4}/(C_\mu \delta) \tag{8b}$$

where α is estimated from the experimental data, and δ is the boundary-layer thickness.

Near the wall, the Couette flow assumption of constant shear stress is made. The standard wall functions based on log law for a smooth wall under zero pressure gradient are used for the parallel velocity component and the turbulent quantities k and ϵ. No attempt was made to take account of the effect of the adverse pressure gradient in the formulation of the wall function.

Grid tests have been carried out with three different mesh sizes (44 × 37, 50 × 42, 65 × 50) to obtain an optimum grid-independent solution in each case. It was found that the solution with the 50 × 42 grids in the X and Y directions were to all purposes grid-independent.

A staggered grid system is employed as in CHAMPION code,[15] in which the velocity components are stored midway

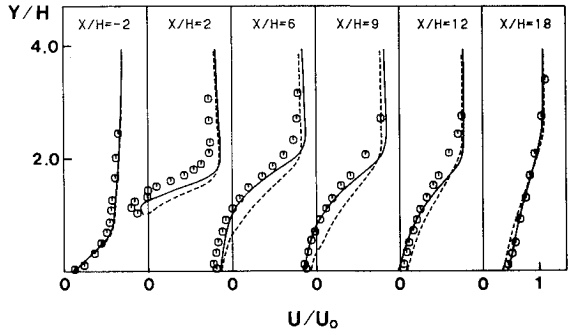

Fig. 2 Comparison of model predictions with the streamwise mean velocity profiles of a thick fence flow (o Moss and Baker[11]; —— present model; --- LRM).

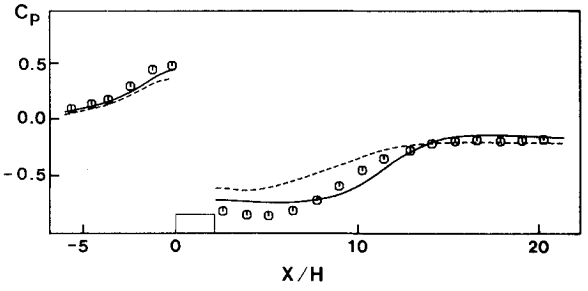

Fig. 3 Comparison of model predictions with the wall static pressure coefficient data of a thick-fence flow (key as for Fig. 2).

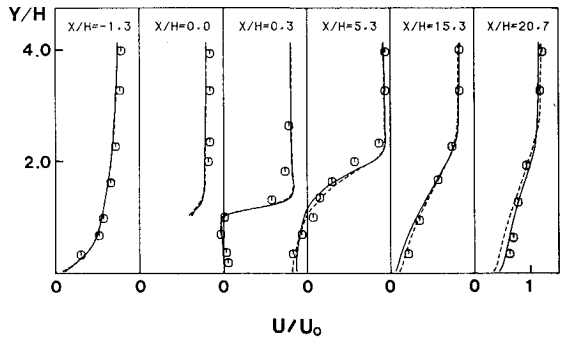

Fig. 4 Comparison of model predictions with the streamwise mean velocity profiles of a thin-fence flow (o Fraser and Siddig[12]; —— present model; --- LRM).

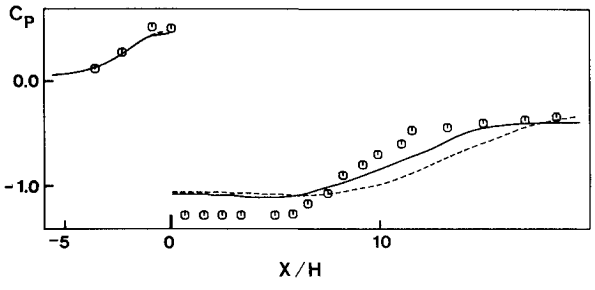

Fig. 5 Comparison of model predictions with the wall static pressure coefficient data of a thin-fence flow (key as for Fig. 4).

between the pressure storage locations. The present solution method employed the SIMPLE algorithm[16] and skew-upwind differential scheme.[17]

Initial field values throughout the computational domain had to be specified properly so as not to cause numerical divergence. The numerical instability is mainly due to the curvature-dependent turbulence model that contains the radius of streamline curvature. This problem was overcome by starting the computation with the standard two-equation model. After the computational flowfield becomes stabilized (after about 200 iterations) with the standard model, the models are switched to curvature-dependent ones.

The computation time of one iteration for 50×42 grid system on an IBM 370 computer was about 8.6 s. When the convergence criterion is such that the summation of residual errors is less than 1% of an inlet total value of the variable, the convergent solution was attained over about 800 iterations.

Results and Discussion

In our preliminary study, currently popular models of Hanjalic and Launder[18] and Leschziner and Rodi,[8] both of whom include curvature correction terms in the model equations, have been tested against the following four flow geometries. The results showed that the latter model yields better overall prediction accuracy, as has been proved by the authors.[8] For clarity, therefore, the present model predictions are to be compared with those of Leschziner and Rodi's model (hereafter referred to as LRM) in the following discussion.

Thick Fence

As a first case study, the thick fence flow (fence width is twice the fence height) by Moss and Baker[11] has been analyzed by using the LRM and present models. The reattachment length predicted by the LRM is $8.3H$, which is about 17% smaller than the experimental result. However, the present model yields it correctly within the experimental uncertainty ($+0.3\%$).

Figure 2 shows the streamwise mean velocity profiles. The location $X/H = -2$ corresponds to the position upstream of the fence, and $0 < X/H < 2$ is the range where the thick normal fence is placed. The locations $X/H = 6$ and 9 are within the recirculating region, and $X/H > 12$ is in the redeveloping region.

The agreement of our prediction with the data is much better than that of the LRM in both the recirculating and redeveloping regions. This shows that the present model is free from the region dependency problem of the previous models. It may be noted that the present model yields fast enough momentum recovery in the redeveloping region.

It seems that the reason for this improvement is mainly due to the length scale adjustment of the present model according to convexity and concavity of the streamline curvature. In the upper part of the separated shear layer above the recirculating region, the length scale is shortened by the increase of the dissipation rate of turbulent kinetic energy caused by the reduction of $C_{\epsilon 2}'$ in the convexly curved streamline curvature field. But in the redeveloping region the length scale is slightly increased due to the opposite mechanism of $C_{\epsilon 2}'$ by the concavely curved streamline curvature.

The calculated wall static pressure distributions are compared with measurements in Fig. 3. Both predictions are good in the upstream of the fence, but in the downstream region the present model yields far better predictions than the LRM, especially in the recirculating region.

Thin Fence

A numerical prediction for a thin-fence flow has been made and compared with the data of Fraser and Siddig.[12] The predicted reattachment length of the LRM is 6.3% shorter than the measured value of $11.2H$, and that of the present model is 8% overpredicted.

Figure 4 represents the streamwise mean velocity profiles. The position of $X/H = 0$ corresponds to the location where a fence is attached to the lower wall. Since thin-fence flow has relatively simple flow characteristics in comparison with thick-fence flow, which yields a complex flow pattern on top of the fence, there is no notable improvement in the present model over the LRM. However, it is noted that the present model permits better momentum recovery in the redeveloping region ($X/H = 20.7$).

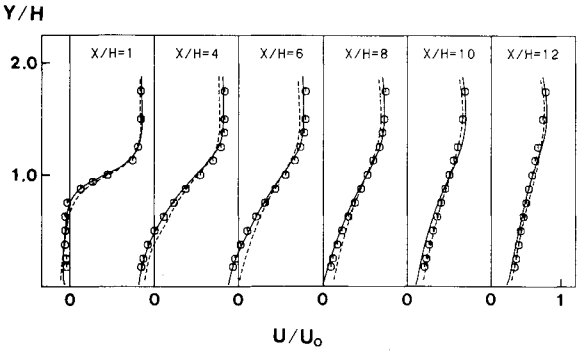

Fig. 6 Comparison of model predictions with the streamwise mean velocity profiles of a backward-facing step flow (o Eaton[13]; —— present model; --- LRM).

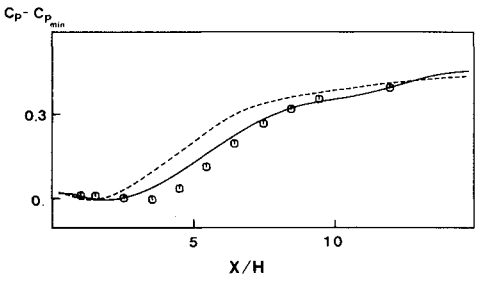

Fig. 7 Comparison of model predictions with the wall static pressure coefficient data of a backward-facing step flow (key as for Fig. 6).

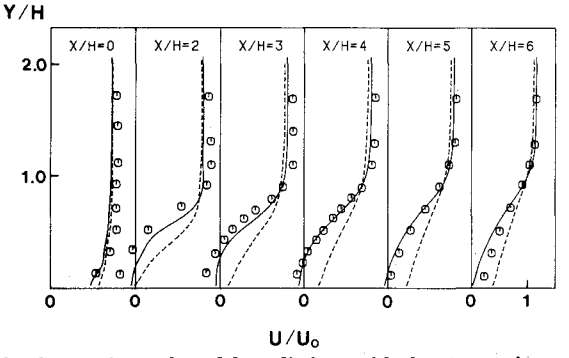

Fig. 8 Comparison of model predictions with the streamwise mean velocity profiles of a front-facing step flow (o Moss and Baker[11]; —— present model; --- LRM).

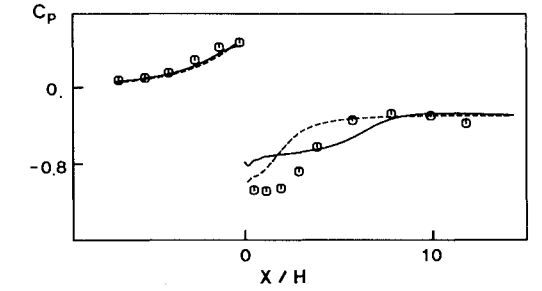

Fig. 9 Comparison of model predictions with the wall static pressure coefficient data of a front-facing step flow (key as for Fig. 8).

The predicted wall static pressure coefficients are shown in Fig. 5. The agreements between both model predictions and experiment are good upstream of the fence. However, the present model yields better prediction downstream of the fence than the LRM.

Backward-Facing Step

The numerical prediction for a backward-facing step flow corresponds to the experiment of Eaton.[13] The predicted reattachment length of the LRM is $6.34H$, whereas the measured value is $7.95H$. The present model yields a reattachment length of $8.03H$, which is very close to the experimental result.

Figure 6 represents the streamwise mean velocity profiles. The position of X/H is measured from the edge of the step wall. On the whole, the present model yields better results than the LRM, especially for the predicted velocity profiles at the positions of $X/H = 4$ and 6 in the recirculating region, which fit the experimental data considerably better. Figure 7 shows the comparison of the wall static pressure coefficients with predictions and measurement. Also, in this case, the prediction of the present model is better than that of the LRM.

Front-Facing Step

Predicted mean velocity profiles on the top of a front-facing step are compared with the experiment of Moss and Baker[11] in Fig. 8, where the position $X/H = 0$ corresponds to the edge of the step. The prediction of the present model is much better than that of the LRM. Such improvement of the prediction accuracy can also be found in the calculation of the reattachment length. Although the predicted length with the LRM is $2.15H$, the present model yields $5.32H$, which is slightly larger than the measured value of $4.7H$.

Figure 9 shows the wall static pressure distribution of the front-facing step flow. In contrast to the good prediction accuracy at the upstream of the step, both prediction results on top of the step are poor. Considering overall prediction accuracy of the static pressure fields by our model in the previous three cases, the cause of such poor agreement in Fig. 9 is not clearly understood.

Conclusions

Incorporation of the new curvature-dependent third-order model in the k and ϵ equations with a curvature-dependent viscous destruction term in the ϵ equation is found to yield very good prediction accuracy for various turbulent recirculating flows.

The prediction of streamwise mean velocities in a thick-fence flow by our model yields much better agreement with the data than that of Leschziner and Rodi's model; especially in the recirculation region, the improvement in prediction accuracy is remarkable. In the thin-fence flow, the present model yields fast enough momentum recovery in the redeveloping region. Significant improvement of the prediction accuracy of the mean velocities was obtained in the front-facing step flow, particularly in the recirculating zone on top of the front-facing step. Therefore, it can be concluded that the present model yields much better prediction accuracy of the mean velocity distributions, not only in the recirculating region but also in the redeveloping region. The wall static pressure coefficient distributions are also better predicted by the present model in all cases. From the foregoing discussion, it is concluded that the present model overcomes the barrier of region dependency of previous turbulence models. This is certainly due to correct representation of the dependency of the decay rate and the third-order spatial transport mechanism on the streamline curvature.

References

[1]Sindir, M. M., "Effects of Expansion Ratio on the Calculation of Parallel-Walled Backward-Facing Step Flows: Comparison of Four Models of Turbulence," American Society of Mechanical Engineers, Paper 83-FE-10, July 1983.

[2]Amano, R. S. and Goel, P., "Computations of Turbulent Flow Beyond Backward-Facing Steps Using Reynolds-Stress Closures," *AIAA Journal*, Vol. 23, Sept. 1985, pp. 1356–1361.

[3]Smits, A. J., Young, S. T. B., and Bradshaw, P., "The Effects of Short Regions of High Surface Curvature on Turbulent Boundary Layers," *Journal of Fluid Mechanics*, Vol. 94, Sept. 1979, pp. 209–242.

[4]Hoffman, P. H., Muck, K. C., and Bradshaw, P., "The Effect of

Concave Surface Curvature on Turbulent Boundary Layers," *Journal of Fluid Mechanics,* Vol. 161, Dec., pp. 371–403.

[5]Castro, I. P. and Bradshaw, P., "The Turbulence Structure of a Highly Curved Mixing Layer," *Journal of Fluid Mechanics,* Vol. 73, Jan. 1976, pp. 265–304.

[6]Durst, F. and Rastogi, A. K., "Turbulent Flow over Two-Dimensional Fences," *Turbulent Shear Flows,* Vol. 2, Springer-Verlag, New York, 1980, pp. 218–232.

[7]Militzer, J., Nicoll, W. B., and Alpay, J. A., "Some Observations on the Numerical Calculation of the Recirculation Region of Twin Parallel Symmetric Jet Flow," *Proceedings of the Symposium on Turbulent Shear Flows,* Pennsylvania State Univ., University Park, PA, 1977, pp. 18.11–18.18.

[8]Leschziner, M. A. and Rodi, W., "Calculation of Annular and Twin Parallel Jets Using Various Discretization Schemes and Turbulence-Model Variations," *Journal of Fluids Engineering,* Vol. 103, June 1981, pp. 352–360.

[9]Benodekar, R. W., Goddard, A. J. H., Gosman, A. D., and Issa, R. I., "Numerical Prediction of Turbulent Flow over Surface-Mounted Ribs," *AIAA Journal,* Vol. 23, March 1985, pp. 359–366.

[10]Gooray, A. M., Watkins, C. B., and Aung, W., "Improvements to the k-ϵ Model for Calculations of Turbulent Recirculating Flow," *Proceedings of the Symposium on Turbulent Shear Flows,* Univ. of Karlsruhe, Karlsruhe, FRG, 1985, pp. 18.26–18.31.

[11]Moss, M. D. and Baker, S., "Recirculating Flows Associated with Two-Dimensional Steps," *Aeronautical Quarterly,* Pt. 3, Aug. 1980, pp. 151–172.

[12]Fraser, M. and Siddig, M. H., "Turbulent Flow over a Plane Normal Wall," *Journal of Mechanical Engineering Science,* Vol. 22, No. 4, 1980, pp. 207–211.

[13]Eaton, J. K., "Turbulent Flow Reattachment: An Experimental Study on the Flow and Structure behind a Backward-Facing Step," Ph.D. Thesis, Stanford Univ., Stanford, CA, 1980.

[14]Chung, M. K., Park, S. W., and Kim, K. C., "Curvature Effect on Third-Order Velocity Correlations and Its Model Representations," *Physics of Fluids,* Vol. 30, March 1987, pp. 626–628.

[15]Pun, W. M. and Spalding, D. B., "A General Computer Program for Two-Dimensional Elliptic Flows," Mechanical Engineering Dept., Imperial College, London, Rept. HTS/76/2, 1976.

[16]Patankar, S. V., "Numerical Heat Transfer and Fluid Flow," McGraw-Hill, New York, 1980, pp. 126–129.

[17]Raithby, G. D., "A Critical Evaluation of Upstream Differencing Applied to Problems Involving Fluid Flow," *Computer Methods in Applied Mechanics and Engineering,* Vol. 9, No. 2, Oct. 1976, pp. 153–164.

[18]Hanjalic, K. and Launder, B. E., "Sensitizing the Dissipation Equation to Irrotational Strains," *Journal of Fluids Engineering,* Vol. 102, March 1980, pp. 34–40.